

Synthesis of Thermally Stable χ -Alumina by Thermal Decomposition of Aluminum Isopropoxide in Toluene

Okorn Mekasuwandumrong,^{†,§} Hiroshi Kominami,^{*,†,¶} Piyasan Praserttham,[‡] and Masashi Inoue^{*,†}

Department of Energy and Hydrocarbon Chemistry, Graduate School of Engineering, Kyoto University, Kyoto 606-8501, Japan

Department of Chemical Engineering, Faculty of Engineering, Chulalongkorn University, Bangkok 10330, Thailand

Thermal decomposition of aluminum isopropoxide in toluene at 315°C resulted in χ -alumina that had high thermal stability, whereas the reaction at lower temperatures resulted in formation of an amorphous product. The χ -alumina thus obtained directly transformed to α -alumina at ~1150°C, bypassing the other transition alumina phases, whereas the amorphous product transformed to γ -alumina and then to θ -alumina before final transformation to α -alumina. When the χ -alumina, solvothermally synthesized at 315°C, was recovered by the removal of the solvent at the reaction temperature, thermal stability of the product was improved further. This procedure is convenient because it avoids bothersome work-up processes that yield large-surface-area and large-pore-volume alumina.

I. Introduction

MANY industrial solid catalysts are made up of active centers anchored on supports that have high porosity, large surface area, and good mechanical strength as well as sufficient thermal stability.¹ Transition aluminas are most widely used in industry as support materials, because a variety of aluminas that have these requisites are commercially available.²

Boehmite is one of the polymorphs of Al(OH). So-called pseudoboehmite is microcrystalline boehmite that has extra water content because of surface hydroxyl groups^{3–5} and is widely used as a precursor of alumina for catalysis uses. Dehydration of pseudoboehmite yields γ -alumina, which transforms to δ -, then θ -, and finally α -alumina with increasing calcination temperatures.^{3–6} These phase transformations are accompanied by a decrease in surface area and variation of surface properties. The phase transformation of alumina is the cause for the loss of surface area.³ For catalysts used for high-temperature reactions, such as catalytic combustion, damage caused by sintering and phase transformation of alumina must be avoided.^{1,2} Therefore, much attention has been given to improve the thermal stability of alumina supports.

In the literature, direct transformation of low-temperature transition alumina (i.e., γ -, η -, and χ -alumina) to α -alumina without formation of high-temperature transition alumina (i.e., δ -, θ -, and κ -alumina) has been reported. Chou and Nieh¹⁷ have reported that

the nucleation of α -alumina occurs along the {220} crystallographic plane of γ -alumina thin films synthesized by radio-frequency (rf) reactive-sputtering deposition. Johnston *et al.*¹⁸ have reported that γ -alumina prepared by laser ablation of an aluminum target in an oxygen atmosphere directly transforms to α -alumina at 1200°C, and they have suggested that this result is due to the lack of water in the as-synthesized powders. Shek *et al.*¹⁹ have reported that γ -alumina prepared by oxidation of pure aluminum metal transforms directly to α -alumina at 1370 K. They have attributed this result to facilitation of nucleation of α -alumina by the strain relaxation of the transition alumina lattice. Simpson *et al.*²⁰ have reported that γ -alumina prepared by electron-beam evaporation of alumina onto a sapphire substrate transformed to α -alumina without formation of the other intermediate phases. They have attributed this result to the epitaxial growth of α -alumina on the sapphire substrate. Ogiwara *et al.*²¹ have found that monodispersed, spherical alumina (amorphous) prepared by the controlled hydrolysis of aluminum alkoxide crystallized to γ -alumina at 1000°C, which converted to α -alumina at 1150°C without formation of intermediate phases. It also has been reported that γ -alumina forms by thermal decomposition of aluminum sulfate transformed to α -alumina directly.^{22–24}

χ -alumina is a modification of transition alumina^{3–8} and is characterized by the appearance of a diffraction peak at $d = 0.212$ nm that cannot be explained by the spinel structure proposed for other transition aluminas, such as γ - and η -alumina.^{3,8,9} χ -alumina is the dehydrated phase of gibbsite (Al(OH)₃). Dollimore *et al.*¹⁰ have found that χ -alumina is formed by thermal decomposition of aluminum oxalate. Because it has been generally believed that χ -alumina cannot be prepared by routes other than dehydration of gibbsite, it has been concluded that aluminum oxalate has a crystal structure similar to that of gibbsite.

In a previous paper from our group,¹¹ the thermal decomposition of aluminum isopropoxide (AIP) in toluene was examined, and χ -alumina was formed by this reaction, which directly transformed to α -alumina at 1150°C. In this article, we reveal the detailed results for χ -alumina formation and α -alumina transformation. Effect of the product recovery procedure also was examined, and pore structures of the thus-obtained products are reported.

II. Experimental Procedures

(1) Sample Preparation

AIP (8 or 25 g) (Nacali Tesque, Kyoto, Japan) was dissolved in 60 mL of toluene (Wako, Osaka, Japan) in a test tube, which served as an autoclave liner, and then the test tube was placed into a 200 mL autoclave. An additional 40 mL of toluene was placed in the gap between the autoclave wall and the test tube. The autoclave was completely purged with nitrogen, heated to a desired temperature at a rate of 2.5°C/min, and maintained at that temperature for 2 h, unless otherwise specified. The reaction temperature was measured using a thermocouple held in the autoclave wall. The

J. E. Blendell—contributing editor

Manuscript No. 10196. Received May 27, 2003; approved April 13, 2004.
Support for O.M. provided by Thailand Research Fund (TRF) and Association of International Education in Japan (AIEJ).

*Member, American Ceramic Society.

†Kyoto University.

‡Chulalongkorn University.

§Visiting student from Chulalongkorn University.

¶Present address: Department of Applied Chemistry, Faculty of Science and Engineering, Kinki University, Osaka 577-8502, Japan.

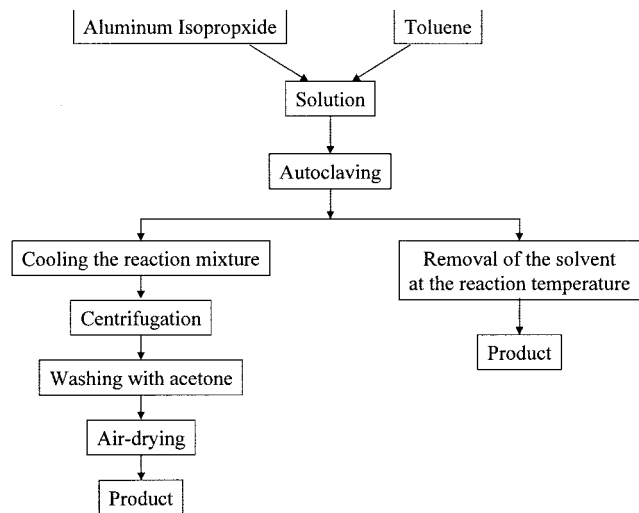


Fig. 1. Processing steps for the preparation of χ -alumina.

actual temperature in the reaction vessel was $\sim 15^\circ\text{C}$ lower than the measured temperature. In some experiments, the reaction mixture was stirred during the reaction. As schematically illustrated in Fig. 1, the reaction product was recovered by two methods. In the first method, after the autoclave was cooled to room temperature, the resulting product was repeatedly washed with acetone by vigorous mixing and centrifuging, and then it was dried in air. In the second method, after the reaction, the autoclave valve was slightly opened and the fluid phase was evaporated at the reaction temperature.^{12,13}

The products recovered by the first method are designated as Al***C*h, where the first three asterisks represent the reaction temperature and the fourth asterisk represents the holding time at the reaction temperature. The product recovered by the second method is specified by adding "P" to the designation. For the products obtained by reaction with stirring, "S" also is added. Therefore, SPAI315C2h means the product obtained by the reaction with stirring at 315°C for 2 h followed by the removal of the solvent at the reaction temperature.

A part of the product was calcined in a box furnace by heating to a desired temperature at a rate of $10^\circ\text{C}/\text{min}$ and holding at that temperature for 30 min.

(2) Characterization

Powder X-ray diffractometry (XRD; Model XD-D1, Shimadzu, Kyoto, Japan) measurements were made using $\text{CuK}\alpha$ radiation and a carbon monochromator. Crystallite size was calculated from the half-height width of a peak at $67.5^\circ 2\theta$ using the Scherrer equation. The composition of the medium after the reaction was analyzed using gas chromatography (Model GC 9A, Shimadzu, Kyoto, Japan) with a FID detector. Specific surface area of the product was calculated using the BET single-point method based on nitrogen uptake measured at 77 K. Nitrogen adsorption isotherms were determined using a gas-sorption system (Model Quantachrome Autosorb-1, Yuasa-Ionics, Tokyo, Japan). Pore-size distribution was calculated using the BJH method with a desorption branch of the isotherm. Thermogravimetric/differential thermal analyses (TGA/DTA) were performed (Model TG-50, Shimadzu, Kyoto, Japan) at a heating rate of $10^\circ\text{C}/\text{min}$ in a 40 mL/min flow of dry air.

III. Results and Discussion

(1) Effect of Reaction Temperature and Holding Time

The XRD patterns of products obtained by the thermal decomposition of AIP in toluene under various conditions are shown in Fig. 2. The Al300C2h product was essentially amorphous,

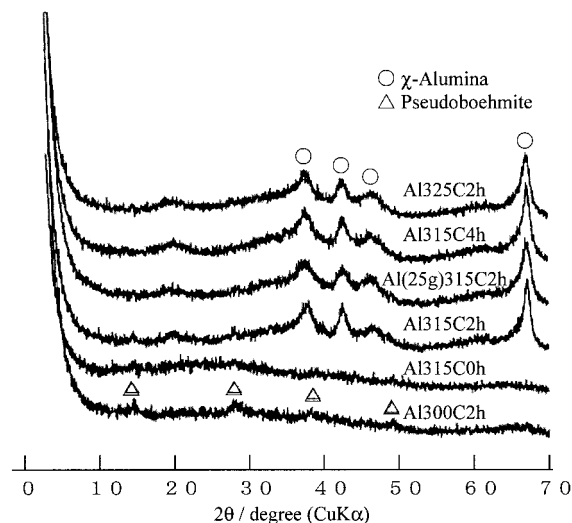
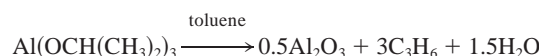


Fig. 2. XRD patterns of the products obtained by thermal decomposition of AIP in toluene under various conditions. Al(25 g)315C2h is the product obtained by charging a large quantity (25 g) of aluminum isopropoxide.

although weak peaks due to pseudoboehmite were observed. On the other hand, the XRD pattern of Al315C2h clearly showed a peak at $2\theta = 42.5^\circ$. This peak corresponded to the prohibited 321 diffraction of the spinel structure and clearly indicated the formation of χ -alumina.^{3,8,9} An amorphous product was obtained when the reaction was quenched just after the autoclave temperature reached 315°C (Al315C0h). This result suggested that crystallization of χ -alumina took place through a solid-state transformation mechanism from the amorphous product deposited from the solution.

To examine the stoichiometry of the reaction, the recovered solvent was analyzed using gas chromatography. Only toluene was detected (no 2-propanol was found), which indicated that the organic moiety of AIP decomposed to propene. Therefore, the overall reaction can be written as follows:



A small amount of water (0.7 mL) intentionally added to the gap between the autoclave wall and the test tube¹⁴ did not affect the formation of χ -alumina, which indicated that the water formed by the reaction did not alter the reaction but presumably facilitated the crystallization of the product. However, addition of a large excess of water resulted in formation of pseudoboehmite.

Physical properties of the as-synthesized products are summarized in Table I. Amorphous products (Al300C2h and Al315C0h) had higher surface areas and lower bulk densities, and they exhibited larger weight losses when compared with the χ -alumina products.

Table I. Physical Properties of Products Obtained by the Thermal Decomposition of AIP in Toluene

Product	BET surface area (m^2/g)	Crystallite size (nm)	Bulk density (g/cm^3)	Ignition loss (%)
Al300C2h	292		0.34	28
Al315C0h	291		0.35	36
Al315C2h	201	10.3	0.6	12
Al325C2h	211	10.7	0.64	18
Al315C4h	213	10.8	0.67	11
Al(25 g)315C2h [†]	244	9.9	0.6	16

[†]Product obtained by the reaction of 25 g of aluminum isopropoxide in toluene at 315°C for 2 h.

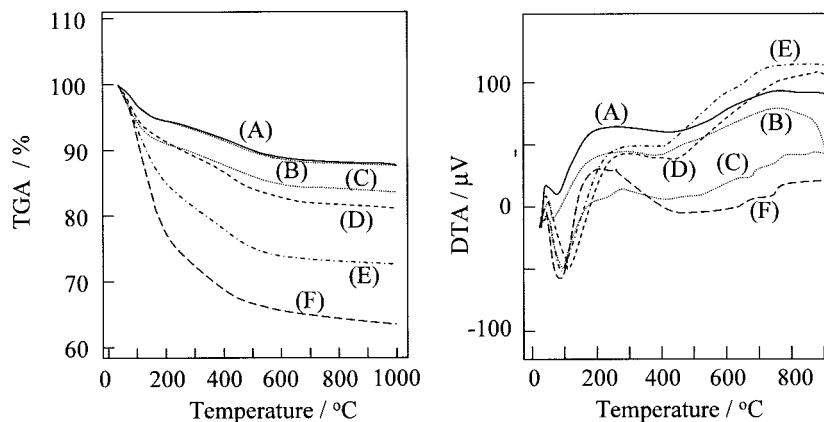


Fig. 3. TG and DTA data of the products: (A) Al₃15C₄h; (B) Al₃15C h; (C) Al(25 g)315C₂h; (D) Al₃25C₂h; (E) Al₃15C₀h; and (F) Al₃00C₂h.

Surface areas and crystallite sizes of the latter products fell within a relatively narrow range irrespective of the reaction conditions.

If the primary particle of χ -alumina is a sphere that has a diameter identical to the crystallite size (10 nm) and if the true density of χ -alumina is 3.0, then the specific surface area of the sphere is calculated to be 200 m²/g. This value is in good agreement with the observed surface areas of the products, which indicates that each primary particle (crystallite) of the product exposes its entire surface to the adsorbate molecules (nitrogen).

Results of thermal analyses of the products are shown in Fig. 3. Two weight-loss processes were detected, both of which were accompanied by endothermic peaks in DTA. The first weight-loss was observed at <160°C and was due to the desorption of physisorbed water. The second weight loss occurred at 300°–600°C and was attributed to the dehydration of surface hydroxyl groups, because the IR spectra of the products (data not shown) showed no indication of the presence of organic moieties. We assumed that the whole surface (200 m²/g) of the product was covered with surface hydroxyl groups, each of which occupied

7.8×10^{-2} nm² (calculated from the cell dimension of gibbsite). Therefore, the weight loss caused by the dehydration of the surface hydroxyl groups that yielded surface anion vacancies and surface oxide ions was calculated to be 3.83%. The observed weight loss at 300°–600°C was 4.2%–5.6% and exceeded the calculated value. Therefore, the products seemed to contain structural hydroxyl groups or strongly bound chemisorbed water.

The XRD patterns of Al₃00C₂h calcined at various temperatures are shown in Fig. 4. The peak at 42.5° 2 θ was not observed during the thermal transformation of the amorphous products, which indicated that crystallization in the inert organic solvent was essential for the formation of χ -alumina.

Figure 5 shows the XRD patterns of Al₃15C₄h calcined at various temperatures. Direct phase transformation of χ -alumina to α -alumina started at ~1100°C and essentially completed at 1150°C. A small amount of θ -alumina was detected for the sample calcined at 1150°C, and this phase seemed to be formed from contaminated pseudoboehmite or amorphous alumina. Al₃15C₂h exhibited phase transformation behavior similar to that of Al₃15C₄h.

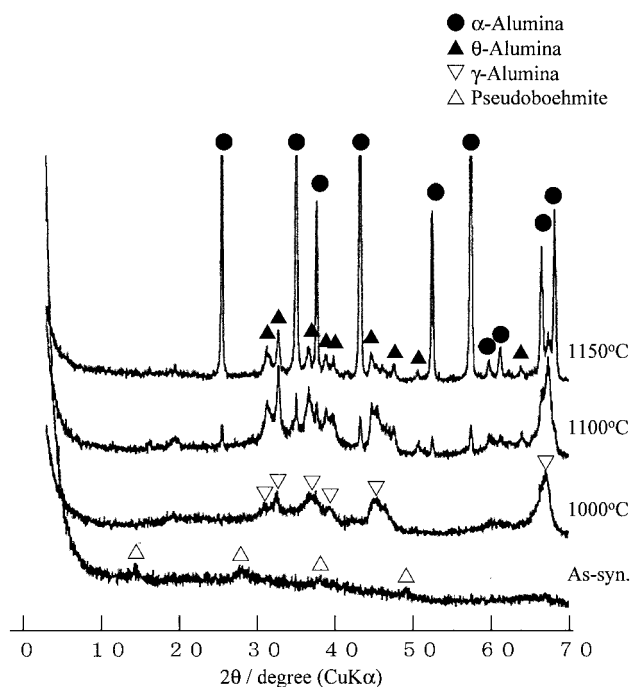


Fig. 4. XRD patterns of the product obtained by the thermal decomposition of AIP in toluene at 300°C for 2 h (Al₃00C₂h) and the samples obtained by calcination thereof at various temperatures.

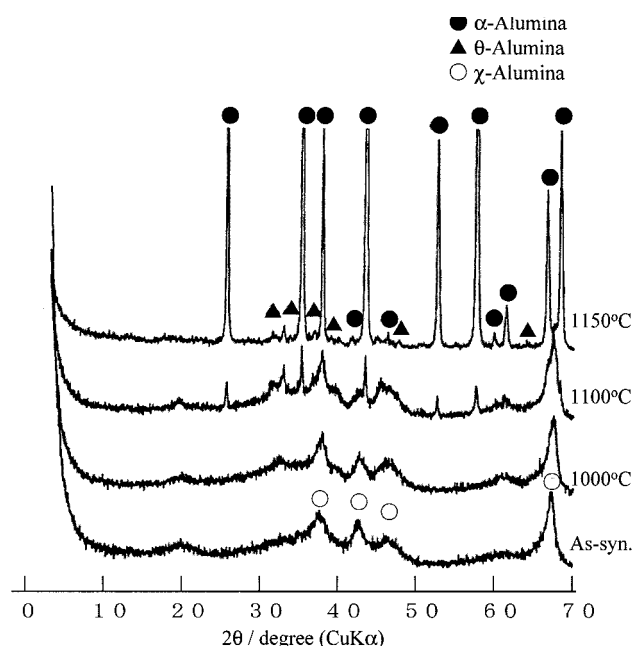
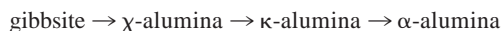


Fig. 5. XRD patterns of the product obtained by the thermal decomposition of AIP in toluene at 315°C for 4 h (Al₃15C₄h) and the samples obtained by calcination thereof at various temperatures.

Table II. BET Surface Areas of the Samples Obtained by Calcination of the Products at Various Temperatures

Product	Phase	Surface area (m ² /g)			
		As-synthesized	1000°C	1100°C	1150°C
Al300C2h	Amorphous	292	117	47	25
Al315C0h	Amorphous	291	107	55	10
Al315C2h	χ-alumina	201	137	85	11
Al325C2h	χ-alumina	211	105	75	43
Al315C4h	χ-alumina	213	100	80	15

In general, χ-alumina obtained by the dehydration of gibbsite (<200 nm) transformed to α-alumina through κ-alumina:^{3–8}



However, χ-alumina obtained by the thermal decomposition of AIP in toluene transformed to stable α-alumina directly, bypassing the formation of the high-temperature transition alumina, i.e., κ-alumina.

Although we cannot draw a common feature for the aluminas that directly transform to α-alumina, the following two points are addressed.

(1) Except for those formed from aluminum sulfate, the transition aluminas that exhibited direct transformation to α-alumina were prepared from aluminum metal or alkoxides, and, therefore, they were free of foreign ions.

(2) γ-alumina crystallized at high temperatures had a tendency to transform to α-alumina without formation of high-temperature transition aluminas.

The first point can be explained using either a thermodynamics or a kinetics reason. When foreign ions thermodynamically destabilize the low-temperature transition alumina structure, transformation to high-temperature transition aluminas does not occur at lower temperatures. Foreign ions may facilitate the nucleation of high-temperature transition aluminas, and this is kinetic enhancement of the formation of high-temperature transition aluminas. On the other hand, absence of foreign ions can disturb the crystallization of high-temperature transition alumina, which thereby facilitates direct crystallization of α-alumina. For the second point, γ-alumina that crystallizes at higher temperatures contains a lesser number of crystal defects than that crystallized at lower temperatures, because sufficient thermal energy is supplied at the crystallization stage. This also lowers the energy level of the transition alumina and prohibits the formation of high-temperature transition aluminas.

Gibbsite is usually contaminated with a small amount of Na⁺ ions,^{3,4} and thermal dehydration of gibbsite that yields χ-alumina cannot eliminate the Na⁺ ions from the matrix. Therefore, the χ-alumina exhibits very broad peaks in the XRD pattern because of the low crystallinity and many defects in the structure. These defects in the χ-alumina structure may promote the formation of κ-alumina. On the other hand, χ-alumina obtained by the thermal decomposition of AIP in toluene is not contaminated with Na⁺ ions. Moreover, the presence of a small amount of water in the solvothermal reaction possibly increases the crystallinity of the product. These situations stabilize the χ-alumina structure and disturb the formation of κ-alumina, which facilitates direct transformation to α-alumina.

The BET surface areas of the calcined products are summarized in Table II. Although the BET surface areas of the amorphous products (Al300C2h and Al315C0h) were higher than those of the χ-alumina products, they rapidly decreased, and ~50 m²/g of the surface area remained when the products were calcined at 1100°C. On the other hand, Al325C2h exhibited higher thermal stability and maintained a BET surface area of 85 m²/g after calcination at the same temperature.

It is generally believed that the α transformation occurs by the nucleation and growth mechanism.^{25–27} Although phase transformation of an oriented γ-alumina film has been reported to proceed by a topotactic process,¹⁷ this result is considered to be a rather special case,^{9,28} because topotactic transformation of transition aluminas in powder or pellet form never has been reported. Because formation of α-alumina from transition alumina requires rearrangement of a cubic oxygen-sublattice to a hexagonal oxygen-sublattice, a large activation energy is required. Nucleation of α-alumina is the rate-determining step, and explosive crystal growth follows.^{25–27} Because of the rapid crystal growth that accompanies α-alumina transformation, the surface area of the product calcined at 1150°C abruptly decreases, as shown in Table II.

Imamura *et al.*²⁹ have compared the catalytic activities of χ-alumina prepared by the present method and γ-alumina prepared by the hydrolysis of AIP, and they have found that these two catalysts have essentially identical activities for the isomerization of 1-butene, although the latter material has a higher surface area (261 m²/g). Moreover, they have reported that calcinations at 1000°C of the χ-alumina maintain 56% of the surface area of the as-synthesized product, while that of the γ-alumina decreases to 37%.²⁹ This result is reasonable, because the former compound does not suffer from the phase transformation, whereas the latter transforms to high-temperature transition aluminas.

(2) Effect of Product Recovery and Stirring

The XRD patterns of the products obtained from the reaction of AIP in toluene at 315°C with stirring (SAI315C2h) and/or with the removal of the solvent at the reaction temperature (SPA1315C2h and SAI315C2h) showed that all the products were χ-alumina. The physical properties of the products are summarized in Table III. When the solvent was removed at the reaction temperature, the BET surface area slightly increased, and the total pore volume significantly decreased and bulk density of the product decreased. These results were attributed to the fact that this procedure avoided coagulation of the particles caused by surface tension of the liquid remaining among the particles,³⁰ which took place during the drying stage of the ordinary procedure.

Although the reaction temperature (315°C) was slightly lower than the critical point of toluene (318°C), the fluid near the critical point was similar to that of the supercritical fluid, and, therefore, this product recovery procedure was considered as a supercritical drying method.^{30,31} Using this procedure, we conducted the solvothermal reaction and supercritical drying in one pot, which avoided bothersome work-up processes and coagulation of the products.^{12,13}

The XRD patterns of SAI315C2h calcined at various temperatures are shown in Fig. 6. The phase transformation started at

Table III. Effect of Stirring and Product Recovery Procedure on the Physical Properties of the As-Synthesized Product Obtained by the Thermal Decomposition of AIP in Toluene

Product	BET surface area (m ² /g)	Crystallite size (nm)	S _t (m ² /g) [†]	Bulk density (g/cm ³)	Total pore volume (cm ³ /g) [‡]	Average pore diameter (nm) [§]	Mode pore diameter (nm)
Al315C2h	201	10.3	203	0.6	0.709	14.1	13.2
SAI315C2h	285	12.4	283	0.57	0.626	8.8	7.4
PAI315C2h	255	8.3	243	0.1	1.899	23.5	
SPA1315C2h	281	9.3	281	0.12	2.321	33.1	

[†]Calculated from the initial slope of the t plot. [‡]Total nitrogen uptake at relative pressure of 0.98. [§]Calculated from total pore volume and BET surface area assuming that the pore is tubular. ^{||}Calculated from the desorption branch of the isotherm using the BJH method.

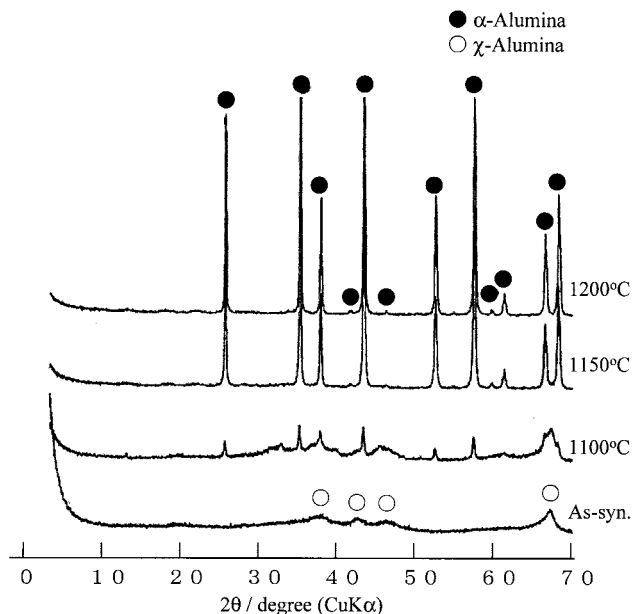


Fig. 6. XRD patterns of the product obtained by the reaction of AIP in toluene with stirring (SAI315C2h) and the samples obtained by calcination thereof at various temperatures.

~1100°C and was completed at 1150°C. θ -alumina was not detected during the phase transformation. This result suggested that SAI315C2h was more homogeneous than AI315C2h. Because the water content in the gas phase was much higher than that in the reaction medium, particles formed near the surface of the medium were affected by the water in the gas phase. Stirring during the reaction avoided this effect, and, therefore, a more homogeneous product was obtained.

BET surface areas of the calcined products are summarized in Table IV. Stirring during the reaction had a minor effect on the physical properties of the calcined products, although SAI315C2h had a larger surface area than AI315C2h. As discussed above, the reaction proceeded by initial formation of an amorphous phase through the deposition from a homogeneous solution followed by transformation to χ -alumina with the aid of adsorbed water. The surface area of the χ -alumina products seemed to be determined by the particle size of the amorphous phase, which was, in turn, determined by the degree of supersaturation of the system. Therefore, stirring little affected the surface areas of the calcined products.

Figure 7 shows the phase transformation behavior of SPAI315C2h. The phase transformation started at ~1150°C and was almost completed at ~1200°C. PAI315C2h showed essentially the same phase transformation behavior as SPAI315C2h. The transformation temperatures of the products obtained by supercritical drying were >50°C higher than those recorded using the ordinary method. This point is discussed later.

Table IV shows that SPAI315C2h and PAI315C2h maintained high surface areas of ~75 m²/g, even after calcinations at 1150°C.

Table IV. Effects of Stirring and Product Recovery Procedure on the BET Surface Areas of Samples Calcined at Various Temperatures

Product	Surface area (m ² /g)				
	As-synthesized	1000°C	1100°C	1150°C	1200°C
AI315C2h	201	137	85	11	7
SAI315C2h	285	132	85	13	8
PAI315C2h	255	142	108	73	10
SPAI315C2h	281	148	115	77	14

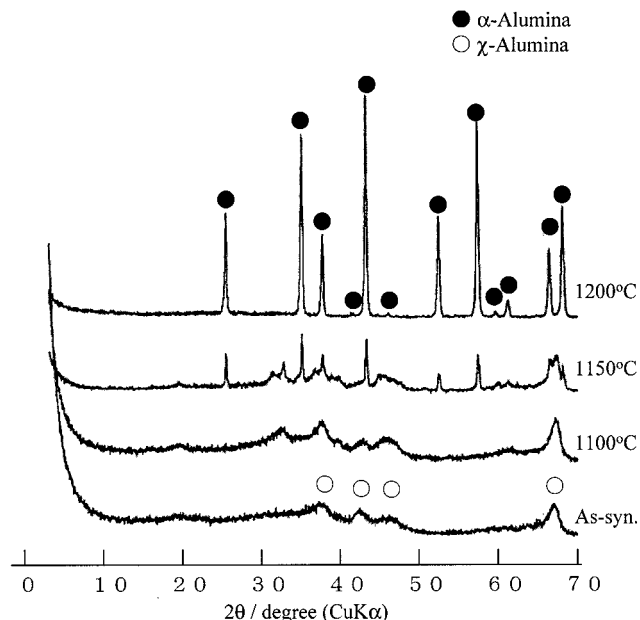


Fig. 7. XRD patterns of the product obtained by the reaction of AIP in toluene with stirring and with the product recovery by the supercritical drying method (SPAI315C2h) and the samples obtained by calcination thereof at various temperatures.

This result was attributed to the fact that these products transformed to α -alumina at higher temperatures.

(3) Morphology of the Products

Scanning electron microscopy results of SPAI315C2h are shown in Fig. 8 and are representative of all the products. The product particles are irregularly shaped and composed of fine primary particles. The other products have similar morphologies.

(4) Pore Structure of the Products

The nitrogen adsorption isotherms (data not shown) of the products recovered by the ordinary method (AI315C2h and SAI315C2h) exhibited a hysteresis-loop characteristic of type E, as classified by de Boer,³² which was explained by the presence of tabular or ink-bottle pores of varying radius.³² Because this type of hysteresis loop is commonly observed for spheroidal cavities or voids between close-packed spherical particles, the observed hysteresis loop seemed to be due to

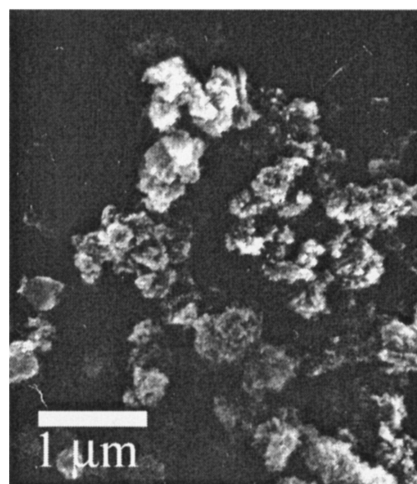


Fig. 8. Scanning electron micrograph of SPAI315C2h.

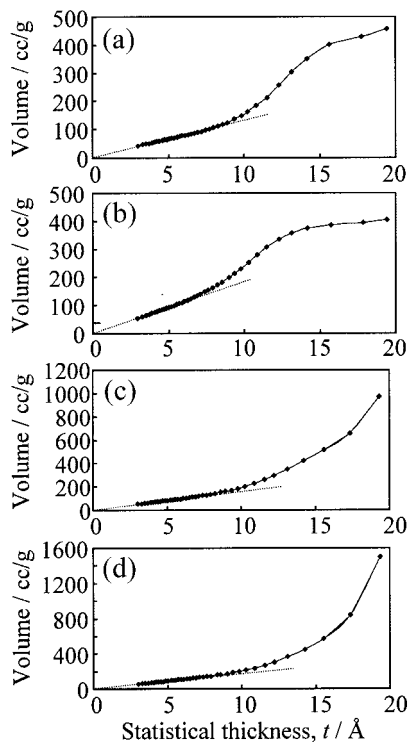


Fig. 9. t plots of (a) Al315C2h, (b) SA1315C2h, (c) PA1315C2h, and (d) SPA1315C2h.

capillary condensation into the voids between the primary particles of χ -alumina.

The t plots^{33,34} derived from the isotherm are presented in Fig. 9. In all the cases, the first part of the plot was a straight line going through the origin, and, from the slope of the line, total surface area, S_t , could be calculated. When a sample had a micropore system, an abrupt decrease in the slope was detected.^{33,34} The present products showed no sign of a decrease in the slope in the t plots, which indicated the absence of a micropore system. Good agreement between S_{BET} and S_t (Table III) also supported this argument. At higher relative pressures (higher t values), deviation from the straight line occurred, because capillary condensation in the mesopore system formed between the primary particles of χ -alumina. The pore-size distributions are shown in Fig. 10.

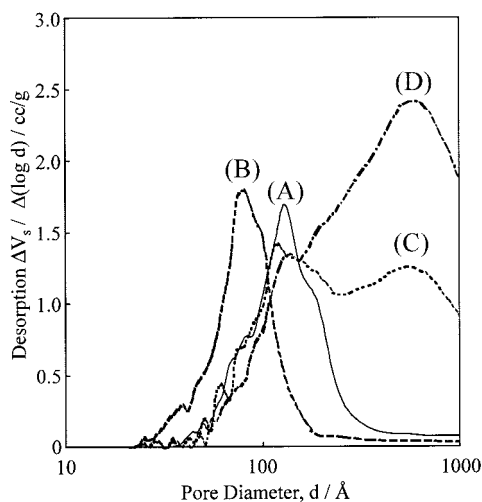


Fig. 10. Pore-size distributions of as-synthesized products: (A) Al315C2h; (B) SA1315C2h; (C) PA1315C2h; and (D) SPA1315C2h.

Al315C2h and SA1315C2h had mode pore diameters in the mesopore range.

When supercritical drying was performed for product recovery, the type-E hysteresis loop disappeared (data not shown), which was ascribed to enlargement of pore sizes. The mode pore diameters of PA1315C2h and SPA1315C2h (Fig. 10) were much larger than those observed for Al315C2h or SA1315C2h, which indicated that the primary particles were packed quite loosely. The supercritical drying method prevented the coagulation of the primary particles, and, therefore, PA1315C2h and SPA1315C2h had a macropore system that formed between the loosely packed primary particles.

The XRD and BET data showed that the products prepared by one-pot synthesis (PA1315C2h and SPA1315C2h) had higher thermal stabilities. This was explained by the increased pore size and the total pore volume (Table III). Transformation from transition alumina to α -alumina took place through a nucleation and growth mechanism,^{25–27} and it was generally believed that nucleation occurred at the contact point between the particles.¹⁹ Because the product obtained using supercritical drying had a lesser number of contact points, the transformation to α -alumina required higher temperature. Moreover, mass transfer for a long distance was required for the sintering of these products, which also contributed to their thermal stabilities.³⁵

Although sintering of the particles inevitably occurs, thermal treatment of the present products causes a relatively small decrease in the surface area, because the particles do not suffer from the phase transformation to high-temperature transition aluminas. Therefore, the present product has a potential use as a catalyst material for use at relatively high temperatures.

IV. Conclusions

Thermal decomposition of AIP in toluene at 315°C gave χ -alumina, which directly transformed to α -alumina. This transformation behavior of nanocrystalline χ -alumina was attributed to the absence of Na^+ ions and the less defected structure. At lower reaction temperatures, an amorphous product was obtained, from which γ -alumina was formed at lower temperature. The transformation temperature of the χ -alumina products was recovered by the supercritical drying method, which was $>50^\circ\text{C}$ higher than those recovered by washing and drying in air. The former products maintained a surface area $>70 \text{ m}^2/\text{g}$, even after calcination at 1150°C . The increased pore volume and pore size, brought about by the prevention of the coagulation of the alumina particles, contributed to the higher thermal stability of these χ -alumina products.

References

- C. N. Satterfield, *Heterogeneous Catalysis in Practice*. McGraw-Hill, New York, 1980.
- R. K. Oberlander, "Aluminas for Catalysts—Their Preparation and Properties"; in *Applied Industrial Catalysis*. Edited by B. E. Leach. Academic Press, London, U.K., 1984.
- W. H. Gitzen, *Alumina as a Ceramics Material*; pp. 14–54. American Ceramic Society, Columbus, OH, 1970.
- K. Wefers and G. M. Bell, "Oxides and Hydroxides of Alumina," Tech. Paper No. 19, Alcoa, Bauxite, AR, 1972.
- K. Wefers, "Nomenclature, Preparation, and Properties of Aluminum Oxides, Oxide Hydroxides, and Trihydroxides"; in *Alumina Chemicals: Science and Technology Handbook*. Edited by L. D. Hart. American Ceramic Society, Westerville, OH, 1990.
- H. C. Stumpf, A. S. Russell, J. W. Newsome, and C. M. Tucker, "Thermal Transformations of Aluminas and Alumina Hydrates," *Ind. Eng. Chem.*, **42** [7] 1398–403 (1950).
- H. Saalfeld, "Structure Phases of Dehydrated Gibbsite"; pp. 310–15 in *Reactivity of Solids*. Edited by J. H. de Boer. Elsevier, Amsterdam, The Netherlands, 1961.
- G. W. Brindley and J. O. Choe, "The Reaction Series, Gibbsite to chi-Alumina to kappa-Alumina to Corundum," *Am. Mineral.*, **46** [7–8] 771–85 (1961).
- I. Levin and D. Brandon, "Metastable Alumina Polymorphs: Crystal Structures and Transition Sequences," *J. Am. Ceram. Soc.*, **81** [8] 1995–2012 (1998).
- D. Dollimore, J. Dollimore, and P. D. Perry, "The Thermal Decomposition of Oxalates. Part VIII. Thermalgravimetric and X-ray Analysis Study of the Decomposition of Alumina Oxalate," *J. Chem. Soc. A*, [3] 448–50 (1967).

- ¹¹M. Inoue, H. Kominami, and T. Inui, "Thermal Transformation of χ -Alumina Formed by Thermal Decomposition of Aluminum Alkoxide in Organic Media," *J. Am. Ceram. Soc.*, **75** [9] 2597–98 (1992).
- ¹²P. Pratherthdam, M. Inoue, O. Medkasuvandumrong, W. Thanakulrangsang, and S. Phatanasri, "Effect of Organic Solvents on the Thermal Stability of Porous Silica-Modified Alumina Powders Prepared via One Pot Solvothermal Synthesis," *Inorg. Chem. Commun.*, **3** [11] 671–76 (2000).
- ¹³S. Iwamoto, K. Saito, M. Inoue, and K. Kagawa, "Preparation of the Xerogels of Nanocrystalline Titanias by the Removal of the Glycol at the Reaction Temperature after the Glycolthermal Method and Their Enhanced Photocatalytic Activities," *Nano Lett.*, **1** [8] 417–21 (2001).
- ¹⁴M. Inoue, H. Kominami, and T. Inui, "Novel Synthesis Method for Thermally Stable Monoclinic Zirconia. Hydrolysis of Zirconium Alkoxides at High Temperatures with a Limited Amount of Water Dissolved in Inert Organic Solvent from the Gas Phase," *Appl. Catal. A General*, **121** [1] L1–L5 (1995).
- ¹⁵J. J. Fripiat, H. Bosmans, and P. G. Rouxhet, "Proton Mobility in Solids. I. Hydrogenic Vibration Modes and Proton Delocalization in Boehmite," *J. Phys. Chem.*, **71** [4] 1097–11 (1967).
- ¹⁶A. B. Kiss, G. Keresztury, and L. Farkas, "Raman and IR Spectra and Structure of Boehmite (γ -AlOOH), Evidence for the Recently Discarded D_{2h}^{17} Space Group," *Spectrochim. Acta*, **36A**, 653–58 (1980).
- ¹⁷T. C. Chou and T. G. Nieh, "Nucleation and Concurrent Anomalous Grain Growth of α -Al₂O₃ during γ - α Phase Transformation," *J. Am. Ceram. Soc.*, **74** [9] 2270–79 (1991).
- ¹⁸G. P. Johnston, R. Muenchausen, D. M. Smith, W. Fahrenholtz, and S. Foltyn, "Reactive Laser Ablation Synthesis of Nanosize Alumina Powder," *J. Am. Ceram. Soc.*, **75** [12] 3293–98 (1992).
- ¹⁹C. H. Shek, J. K. L. Lai, T. S. Gu, and G. M. Lin, "Transformation Evolution and Infrared Absorption Spectra of Amorphous and Crystalline Nano-Al₂O₃ Powders," *Nanostruct. Mater.*, **8** [5] 605–10 (1997).
- ²⁰T. W. Simpson, Q. Wen, N. Yu, and D. R. Clarke, "Kinetics of the Amorphous \rightarrow γ \rightarrow α Transformation in Aluminum Oxide: Effect of Crystallographic Orientation," *J. Am. Ceram. Soc.*, **81** [1] 61–66 (1998).
- ²¹T. Ogihara, H. Nakagawa, T. Yanagawa, N. Ogata, and K. Yoshida, "Preparation of Monodisperse, Spherical Alumina Powders from Alkoxides," *J. Am. Ceram. Soc.*, **74** [9] 2263–69 (1991).
- ²²D. W. Johnson and F. J. Schnettler, "Characterization of Freeze-Dried Al₂O₃ and Fe₂O₃," *J. Am. Ceram. Soc.*, **53** [8] 440–44 (1970).
- ²³E. Kato, K. Daimon, and M. Nanbu, "Decomposition of Two Aluminum Sulfates and Characterization of the Resultant Aluminas," *J. Am. Ceram. Soc.*, **64** [8] 436–45 (1981).
- ²⁴M. D. Sacks, T.-Y. Tseng, and S. Y. Lee, "Thermal Decomposition of Spherical Hydrated Basic Aluminum Sulfate," *Am. Ceram. Soc. Bull.*, **63** [2] 301–10 (1984).
- ²⁵F. W. Dynys and J. W. Halloran, " α -Alumina Formation in Alum-Derived γ -Alumina," *J. Am. Ceram. Soc.*, **65** [9] 442–48 (1982).
- ²⁶K. J. Morrissey, K. K. Czanderna, C. B. Carter, and R. P. Merrill, "Growth of α -Alumina within a Transition Alumina Matrix," *J. Am. Ceram. Soc.*, **67** [5] C-88–C-90 (1984).
- ²⁷D. S. Tucker, "Gamma-to-Alpha Transformation in Spherical Aluminum Oxide Powders," *J. Am. Ceram. Soc.*, **68** [7] C-163–C-164 (1985).
- ²⁸R. B. Bagwell, G. L. Messing, and P. R. Howell, "The Formation of α -Alumina from θ -Alumina: The Relevance of a 'Critical Size' and Diffusional Nucleation or 'Synchro-Shear'?", *J. Mater. Sci.*, **36** [7] 1833–41 (2001).
- ²⁹S. Imamura, T. Kitao, H. Sasaki, and K. Utani, "Properties of χ -Alumina as Related to Catalysis," *React. Kinet. Catal. Lett.*, **55** [1] 19–24 (1995).
- ³⁰J. N. Armor and E. J. Carlson, "Variables in the Synthesis of Unusually High Pore Volume Aluminas," *J. Mater. Sci.*, **22** [7] 2549–56 (1987).
- ³¹G. M. Pajonk, "Aerogel Catalysts," *Appl. Catal.*, **72** [2] 217–66 (1991).
- ³²J. H. de Boer, *The Structure and Properties of Porous Materials*. Butterworth, London, U.K., 1958.
- ³³B. C. Lippens and J. H. de Boer, "Studies on Pore Systems in Catalysts. I. The Adsorption of Nitrogen, Apparatus, and Calculation," *J. Catal.*, **3** [1] 32–37 (1964).
- ³⁴B. C. Lippens and J. H. de Boer, "Studies on Pore Systems in Catalysts. V. The t Method," *J. Catal.*, **4** [3] 319–23 (1965).
- ³⁵T. Ishikawa, R. Ohashi, H. Nakabayashi, U. Kakuta, A. Ueno, and A. Furuta, "Thermally Stabilized Transitional Alumina Prepared by Flame Pyrolysis of Boehmite Sols," *J. Catal.*, **134** [1] 87–97 (1992). □